

Truncation Correction using a 3D Filter for Cone-beam CT

Yan Xia, Andreas Maier, Frank Dennerlein, and Joachim Hornegger

Abstract—Recently, a novel method for region of interest (ROI) reconstruction from truncated projections with neither the use of prior knowledge nor explicit extrapolation has been published, named Approximated Truncation Robust Algorithm for Computed Tomography (ATRACT). It was derived by analytically reformulating the standard Feldkamp-Davis-Kress (FDK) algorithm into a reconstruction scheme that is by construction less sensitive to lateral data truncation. In this paper, we present and investigate a variation of the ATRACT that is to apply ATRACT in 3D by decomposing the ramp filter into the 3D Laplace filter and a 3D residual filter. ROI reconstruction can be readily realized by performing these two successive filters on projection data stack at once and followed by standard backprojection. Real data evaluation shows that the new method at least performs as well as the native ATRACT in terms of truncation correction. However, for off-center reconstruction, the linear gradient artifact arose in native ATRACT is essentially reduced by the new method.

I. INTRODUCTION

It is well known that the X-ray radiation dose exposed to the patient during a CT exam is proportional to the volume that is irradiated during the scan. Several medical applications require only a small volume to be imaged. For example, in the neurointerventional radiology only micro devices, e.g. implanted stents or coils, are required to be examined in multiple times. Although only the small area is of diagnostic interest, conventionally, a scan with a full field of view (FOV) was performed, resulting in a considerable dose to the patient. Hence, a restriction of the X-ray beam to only that area would significantly reduce radiation dose. This is simply done by deploying a collimator near the X-ray source. However, the resulting lateral truncation in projections, poses a challenge to the conventional tomographic reconstruction algorithms.

So far many algorithms specially concerning the ROI reconstruction have been proposed. Some are based on the requirement of prior knowledge on the reconstructed object so that the ROI problem can be exactly solved [1], [2], [3]. Other approaches estimate the missing data using an extrapolation procedure as a pre-processing step [4], [5], [6], [7].

A novel method (ATRACT) has been suggested for ROI reconstruction with neither the use of prior knowledge nor explicit extrapolation [8]. In this method, the standard ramp filter is decomposed into the 2D Laplace filtering and a 2D Radon-based filtering step or 2D convolution-based filtering.

Y. Xia, A. Maier and J. Hornegger are with the Pattern Recognition Lab, Friedrich-Alexander-University Erlangen-Nuremberg, 91058 Erlangen, Germany. Y. Xia and J. Hornegger are also with the Erlangen Graduate School in Advanced Optical Technologies (SAOT), Friedrich-Alexander-University Erlangen-Nuremberg, 91052 Erlangen, Germany. (e-mail: yan.xia@cs.fau.de; andreas.maier@cs.fau.de; joachim.hornegger@cs.fau.de).

F. Dennerlein is with Siemens AG, Healthcare Sector, 91052 Erlangen, Germany (e-mail: frank.dennerlein@siemens.com).

In this paper, we present and investigate a variation of the original ATRACT that is to apply ATRACT in 3D by decomposing the ramp filter into the 3D Laplace filter and a 3D residual filter. We expect the 3D convolution-based filtering will gain more stability than its 2D counterpart, especially in the truncated edge.

This paper is organized as follows. Section II reviews the ATRACT algorithm and presents new 3D ATRACT algorithm. Experiment setups are specified in section III, and reconstruction results from these setups are presented in section IV. The paper ends with conclusions, in section V.

II. TRUNCATION CORRECTION METHODS

A. 2D ATRACT

Intuitively, the idea behind ATRACT is to adapt the Feldkamp-Davis-Kress (FDK) algorithm [9] by decomposing the 1D ramp filter operation into two successive 2D filtering steps — the 2D Laplace filtering and a 2D Radon-based filtering step — one acting locally and one acting non-locally on the projection data. We refer to this method as 2D ATRACT in the following. In presence of lateral data truncation, 2D ATRACT allows us to exclude the artifacts typically occurring during filtering, simply by removing the singularities (spikes) at the edges of lateral data truncation after the Laplace operation. With the FDK method, such a removal is not straight-forward, due to the non-local character of the ramp filter. In its later version, the Radon-based filter was substituted by a 2D convolution-based filter for increasing computational performance [10], [11]. This naturally inspires the idea of an alternative decomposition of the 1D ramp filter in 3D convolutions, to further improve the image quality.

B. 3D ATRACT

As discussed above, the 3D ATRACT algorithm is also obtained by a modification of the standard ramp filter in FDK algorithm. That is to decompose the ramp filter into the 3D Laplace filter and a 3D residual filter.

Fig. 1 shows the associated notations in the cone-beam short-scan imaging geometry. The mathematical expression of 3D projection data stack $g(\lambda, u, v)$ can be written as follows:

$$g(\lambda, u, v) = \int_0^{\infty} f(\mathbf{a}(\lambda) + t\boldsymbol{\alpha}(\lambda, u, v)) dt, \quad (1)$$

where u, v are flat detector coordinates and λ indicates angular coordinate.

Using the notations that are shown in Fig. 1, the 3D ATRACT algorithm can be written as follows:

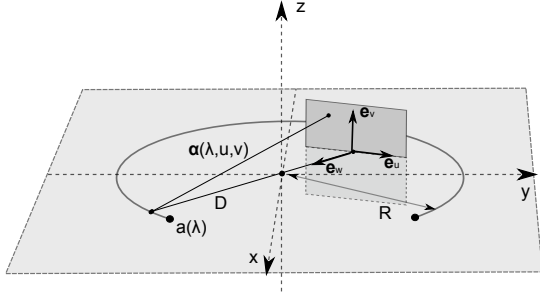


Fig. 1. Cone-beam geometry and associated notation: The curve $\mathbf{a}(\lambda) = (R \cos \lambda, R \sin \lambda, 0)$ describes the trajectory of the X-ray source, with the scan radius R and the rotation angle λ . The planar detector is parallel to the unit vectors $\mathbf{e}_u(\lambda)$ and $\mathbf{e}_v(\lambda)$ and at distance D from the source. $\mathbf{e}_w(\lambda)$ is the detector normal. We use the 3D function $g(\lambda, u, v)$ to describe the projection data stack at the point (u, v) acquired at angle λ .

Step 1: Cosine- and Parker-like weighting of projection data to obtain pre-scaled projection data $g_1(\lambda, u, v)$:

$$g_1(\lambda, u, v) = \frac{Dm(\lambda, u)}{\sqrt{D^2 + u^2 + v^2}} g(\lambda, u, v) \quad (2)$$

where $m(\lambda, u)$ is Parker weight for short-scan data.

Step 2: 3D Laplace filtering to obtain projection data $g_2(\lambda, u, v)$:

$$g_2(\lambda, u, v) = \left(\frac{\partial^2}{\partial \lambda^2} + \frac{\partial^2}{\partial u^2} + \frac{\partial^2}{\partial v^2} \right) g_1(\lambda, u, v) \quad (3)$$

Step 3: 3D convolution-based residual filtering to get filtered projection data $g_F(\lambda, u, v)$:

$$g_F(\lambda, u, v) = \int_{u_1}^{u_2} \int_{v_1}^{v_2} \int_{\lambda_1}^{\lambda_2} g_2(\lambda - \lambda', u - u', v - v') h_{3D}(\lambda', u', v') d\lambda' du' dv' \quad (4)$$

Step 4: 3D cone-beam backprojection to get the estimated object function $f^{(ATRACK)}(x, y, z)$:

$$f^{(ATRACK)}(x, y, z) = \int_{\lambda_1}^{\lambda_2} \frac{RD}{[R - \mathbf{x} \cdot \mathbf{e}_w(\lambda)]^2} g_F(\lambda, u, v) d\lambda \quad (5)$$

where $\mathbf{x} = (x, y, z)$.

As illustrated in Fig. 2, reconstructions from the truncated data can be readily realized by performing two successive 3D filters on pre-scaled 3D projection data stack at once and followed by standard backprojection. Similarly, 3D ATRACT is able to exclude artificial high frequencies (removal of high spikes) after the 3D Laplace filtering step. Unlike the 2D ATRACT, additional removal of the spikes in λ direction is required. That means either removal of the first and last projections or constantly extrapolate them to avoid abrupt changes. Subsequently, the 3D residual filtering is carried out to obtain the desired filtered projections. In practice, the 3D Laplace operation can be achieved using a $3 \times 3 \times 3$ kernel with a different angular weighting in spatial domain. The 3D residual filtering can be implemented by using 3D FFT-based convolution, and the residual kernel in Fourier domain is given by:

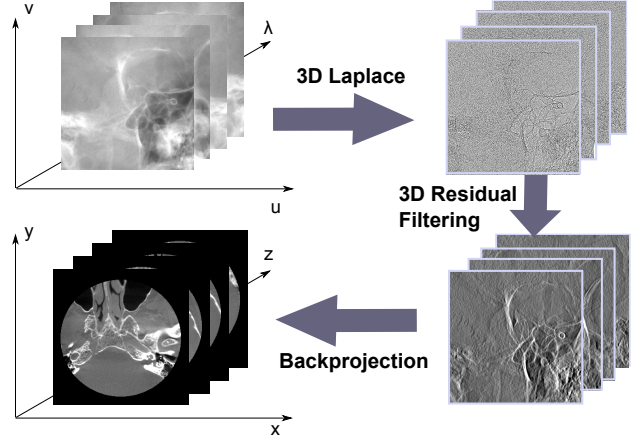


Fig. 2. Illustration of the 3D ATRACT algorithm. ROI reconstruction can be readily realized by performing two successive filters on the data stack at once and followed by the standard backprojection.

$$H_{3D}(\omega_\lambda, \omega_u, \omega_v) = -\frac{|\omega_u|}{\omega_\lambda^2 + \omega_u^2 + \omega_v^2} \quad (6)$$

Also note that discretization in u and v (i.e. du and dv) is identical (square pixels assumed) while discretization in λ differs a lot. Thus, in numerical implementation we choose a different discretization in λ , i.e. $\mu d\lambda$, where $\mu = 0.025$ is a scaling factor.

III. EXPERIMENT SETUP

The proposed algorithm was evaluated by the following datasets in terms of spatial resolution, low contrast resolution as well as robustness of correction quality. All datasets are acquired on a C-arm system (Siemens AG, Healthcare Sector, Forchheim, Germany) and contain 496 projection images (1240×960) with effective pixel size of $0.308 \times 0.308 \text{ mm}^2$ in 2×2 binning mode.

To evaluate the spatial resolution and low contrast resolution of the reconstructions from the new algorithm, we used a Siemens cone-beam phantom that contains several low- and high-contrast inserts useful for evaluation of image quality. We also used two clinical datasets acquired from St. Lukes' Episcopal Hospital (Houston, TX, USA), to quantify the robustness of the truncation correction in practical application.

In the following evaluation, two scenarios were considered. In the baseline scenario, no collimation was applied during the scan, yielding non-truncated projections on the entire area of the detector. In second scenario, we virtually cropped projection images so that only the small region of interest was kept. The non-truncated projections were reconstructed by FDK, which was used as the reference here. The virtually truncated projections, in which only up to 30% of the FOV remained compared to non-truncated projections, were reconstructed by the new algorithm. We also investigated the performance of the 2D ATRACT method, and compared it to the new correction method.

Analogous to the 2D ATRACT algorithm, the new algorithm also suffers from a global volume scaling artifact. A correction of scaling and bias was performed to align the range of values between FDK and the new method.

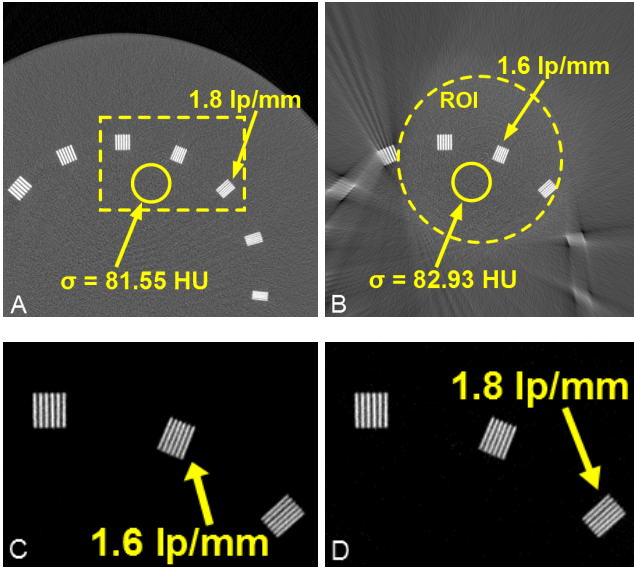


Fig. 3. Reconstruction results of the line-pair inserts phantom. Slice thickness is 0.25mm. A) and C): Standard FDK reconstruction from non-truncated projections, B) and D): 3D ATRACT reconstruction from virtually truncated projections.

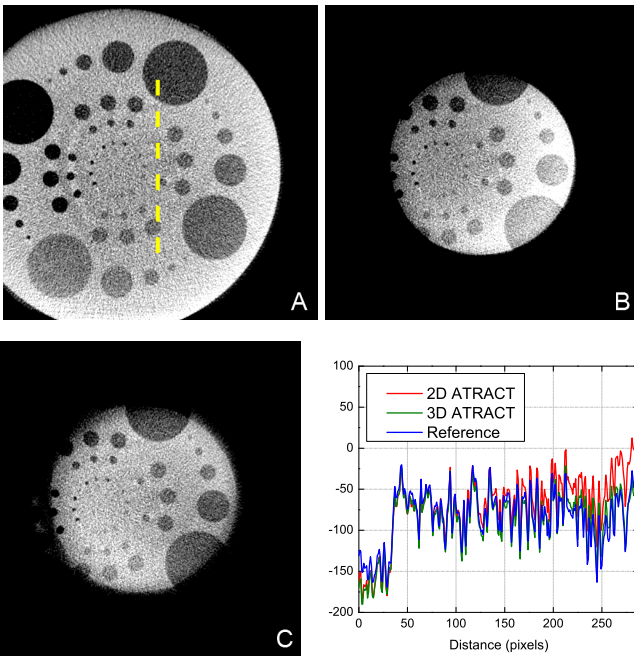


Fig. 4. Reconstruction results of the low contrast inserts in the gray scale window [-200HU, 0HU]. Slice thickness is 0.3mm. A): Standard FDK reconstruction from non-truncated projections, B) and C): 2D ATRACT and 3D ATRACT reconstruction from virtually truncated projections. Line profiles along yellow-dashed line in all methods are also provided.

IV. RESULTS

A. Spatial Resolution and Low Contrast Resolution

Fig. 3 shows the reconstructions of the line-pair phantom. The investigated line-pair inserts (shown in yellow dashed box) in a clockwise direction have modulation of 1.4 lp/mm, 1.6 lp/mm and 1.8 lp/mm, respectively. The noise level of the given slices, estimated by computing the standard deviation

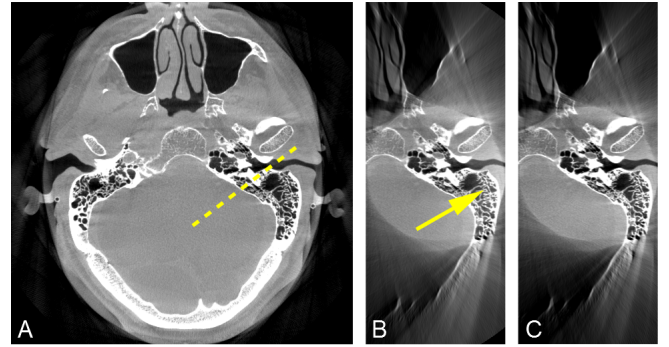


Fig. 6. Transversal slices of the clinical dataset 2 by the three algorithms, in the grayscale window [-1000HU, 1000HU]. Slice thickness is 0.4mm. A): Standard FDK reconstruction from non-truncated projection, B): 2D ATRACT-based ROI reconstruction, C): 3D ATRACT-based ROI reconstruction.

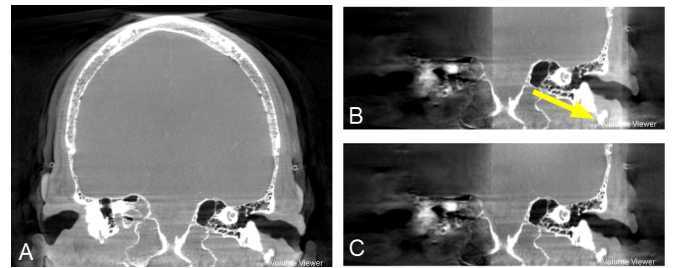


Fig. 7. Coronal slices of the clinical dataset 2 by the three algorithms, in the grayscale window [-1000HU, 1000HU]. Slice thickness is 0.4mm. A): Standard FDK reconstruction from non-truncated projection, B): 2D ATRACT-based ROI reconstruction, C): 3D ATRACT-based ROI reconstruction.

within the yellow cycles, is 81.55 HU for the standard FDK reconstruction, and 82.93 HU for the 3D ATRACT-based ROI reconstruction. The reconstruction results confirm that 3D ATRACT reconstruction yields, for the investigated inserts, identical spatial resolution to the full FOV reconstruction by FDK.

Reconstructions of the low contrast inserts from FDK, 2D ATRACT and 3D ATRACT are represented in Fig. 4. The line profile along the yellow-dashed line in each slices is also given in right bottom. No significant differences are observed between ROI reconstructions and the reference reconstruction in terms of low contrast resolution. We found the result from

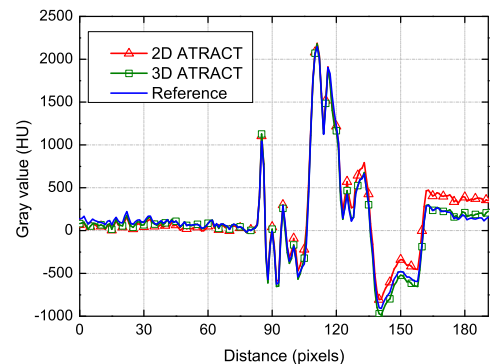


Fig. 8. Profiles along the yellow-dashed line shown in the transversal slices of clinical dataset 2.

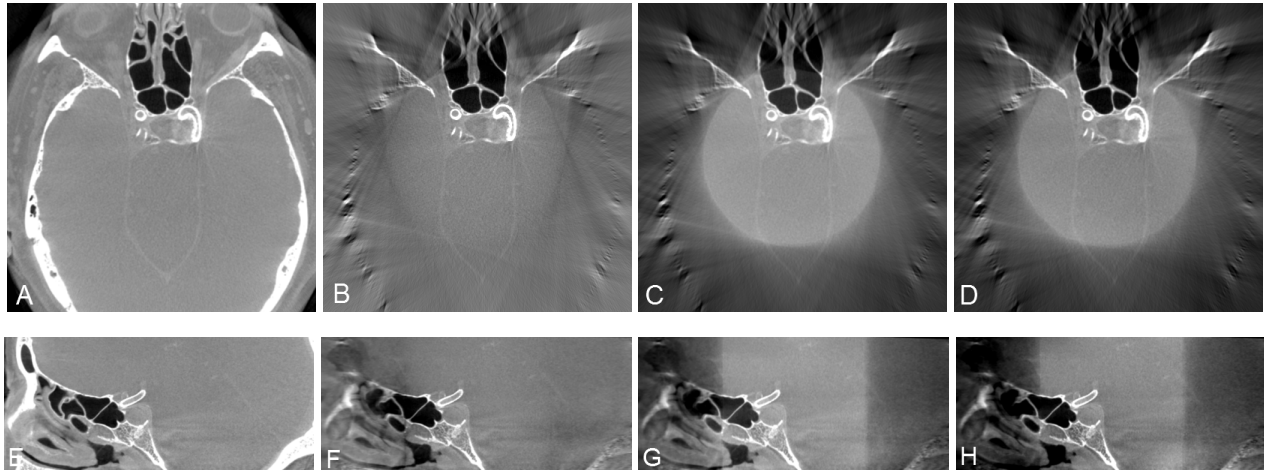


Fig. 5. Reconstruction results of the clinical dataset 1 by the three algorithms, in the grayscale window [-1000HU, 1000HU]. Slice thickness is 0.35mm. A) and E): FDK reconstruction from non-truncated projection, B) and F): constantly extrapolated FDK-based ROI reconstruction, C) and G): 2D ATRACT-based ROI reconstruction, D) and H): 3D ATRACT-based ROI reconstruction.

2D ATRACT avoids the cupping artifact, but comes with a small linear gradient due to off-center reconstruction. Note that such artifacts were also observed in previous work [10]. A better result is obtained by 3D ATRACT that yields a reconstruction close to the reference.

B. Correction Quality

Reconstruction results of the clinical dataset 1 are shown in Fig. 5. It is clear that the straightforward FDK algorithm with a constant extrapolation cannot completely avoid the radial gradient-like truncation artifacts. As opposed to FDK-based ROI reconstruction, satisfying results are obtained by the proposed method and 2D ATRACT. No radial artifacts in the FOV are observed, which implies that truncation artifacts are essentially suppressed by the two methods.

In the clinical dataset 2, we deliberately applied an asymmetric collimation and thus resulted in the off-center ROI reconstruction. Transversal slices are represented in Fig. 6 and coronal slices are in Fig. 7. We observed that the overall correction quality in the reconstruction by both methods is maintained. However, it is noted that intensities tend to increase near the outmost edges of the 2D ATRACT reconstruction (shown by the arrows in Fig. 6(B) and Fig. 7(B)) while not observed in 3D ATRACT. The profiles along the yellow-dashed line shown in Fig. 8 also demonstrate this observation.

V. CONCLUSION

In this paper, we presented a novel method that adapts the previously suggested ATRACT method in three dimensional by decomposing the standard ramp filter into the 3D Laplace filter and a 3D convolution-based filter. As opposed to the native ATRACT, the new method is able to handle the off-center ROI reconstruction caused by an asymmetric collimation. However, the 3D convolution is more computationally demanding than its 2D counterpart, which would consequently affect the reconstruction speed.

ACKNOWLEDGMENT

The authors gratefully acknowledge funding by Siemens AG, Healthcare Sector and of the Erlangen Graduate School in Advanced Optical Technologies (SAOT) by the German Research Foundation (DFG) in the framework of the German excellence initiative. The concepts and information in this paper were never submitted, published, or presented before.

REFERENCES

- [1] F. Noo, R. Clackdoyle, and J. D. Pack, "A Two-step Hilbert Transform Method for 2D Image Reconstruction," *Physics in Medicine and Biology*, vol. 49, no. 17, pp. 3903–3923, 2004.
- [2] X. Pan, Y. Zhou, and D. Xia, "Image reconstruction in peripheral and central region-of-interest and data redundancy," *Medical Physics*, vol. 32, no. 3, pp. 673–684, 2005.
- [3] H. Kudo, M. Courdurier, F. Noo, and M. DeFRise, "Tiny a priori knowledge solves the interior problem in computed tomography," *Physics in Medicine and Biology*, vol. 52, no. 9, p. 2207, 2008.
- [4] B. Ohnesorge, T. Flohr, K. Schwarz, J. P. Heiken, and J. P. Bae, "Efficient correction for CT image artifacts caused by objects extending outside the scan field of view," *Medical Physics*, vol. 27, no. 1, pp. 39–46, 2000.
- [5] J. Hsieh, E. Chao, J. Thibault, B. Grekowitz, A. Horst, S. McOlash, and T. J. Myers, "A novel reconstruction algorithm to extend the CT scan field-of-view," *Medical Physics*, vol. 31, no. 9, pp. 2385–2391, 2004.
- [6] J. D. Maltz, S. Bose, H. P. Shukla, and A. R. Bani-Hashemi, "CT truncation artifact removal using water-equivalent thicknesses derived from truncated projection data," in *IEEE Engineering in Medicine and Biology Society*, pp. 2905–2911, 2007.
- [7] A. Maier, B. Scholz, and F. Dennerlein, "Optimization-based Extrapolation for Truncation Correction," in *2nd CT Meeting*, pp. 390–394, 2012.
- [8] F. Dennerlein, "Cone-beam ROI reconstruction using the Laplace operator," in *Proceedings of Fully 3D 2011*, pp. 80–83, 2011.
- [9] L. A. Feldkamp, L. C. Davis, and J. W. Kress, "Practical cone beam algorithm," *Optical Society of America*, vol. 1, pp. 612–619, 1984.
- [10] F. Dennerlein and A. Maier, "Region-of-interest reconstruction on medical C-arms with the ATRACT algorithm," in *Proceedings of SPIE*, p. 83131B, 2012.
- [11] Y. Xia, A. Maier, F. Dennerlein, H. G. Hofmann, and J. Hornegger, "Efficient 2D filtering for cone-beam VOI reconstruction," in *IEEE NSS-MIC*, pp. 2415–2420, 2012.